ISSN 1070-3284, Russian Journal of Coordination Chemistry, 2022, Vol. 48, No. 4, pp. 250–259. © Pleiades Publishing, Ltd., 2022.

Three Compounds Constructed from 2-Chloro-4-ferrocenylbenzoate and N-Containing Ligands: Synthesis, Crystal Structures, and Microbiological Studies

S. M. Wang[a, b], J. H. Hao[b, c, *], Y. Z. Tang[b], X. L. Sun[d], F. S. Zhou[a, b], Z. Y. Liu[b], Y. Zhu[b], and J. P. Li[b, **]

[a] *College of Chemical Engineering and Printing-Dyeing Engineering, Henan University of Engineering, Henan, 451191 P.R. China*

[b] *College of Chemistry, Zhengzhou University, Henan, 450052 P.R. China*

[c] *Faculty of Science, Henan University of Animal Husbandry and Economy, Henan, 450046 P.R. China*

[d] *Henan Province Medical Instrument Testing Institute, Henan, 450018 P.R. China*

**e-mail: zzmzhjh@126.com*

***e-mail: ljp-zd@163.com*

Received July 7, 2021; revised August 22, 2021; accepted August 22, 2021

Abstract—Self-assemblies of the flexible ferrocenyl 2-chloro-4-ferrocenylbenzoate with Cd^{2+}cations in the presence of N-containing ligands result in three compounds, namely, $[Cd(\eta^1\text{-}OOCClH_3C_6Fc)(\eta^2\text{-}OOCClH_3C_6Fc)(Phen)(H_2O)]$ (**I**), $[Cd(\eta^2\text{-}OOCClH_3C_6Fc)_2(2,2'\text{-bipy})]$ (**II**) and $[(HOOCClH_3C_6Fc)_2(4,4'\text{-bipy})]$ (**III**) (Fc = $(\eta^5\text{-}C_5H_4)Fe(\eta^5\text{-}C_5H_5)$, phen = 1,10-phenanthroline, 2,2'-bipy = 2,2'-bipyridine, 4,4'-bipy = 4,4'-bipyridine). Their structures have been determined by single-crystal X-ray diffraction analyses (CIF files CCDC nos. 1874492 (**I**), 1874493 (II), 1874494 (**III**)) and further characterized by elemental analyses, IR spectra. Crystallographic characterization shows that both **I** and **II** are mononuclear complexes exhibiting the 0D structures, while compound **III** gives a supramolecular structure. Notably, various C–H···π interactions and C–H···Cl interactions are discovered in **I**–**III**, and they have significant contributions to self-assembly, which extend mononuclear structures to infinite 3D supramolecular networks. Moreover, the microbiological properties of **I**–**III** were studied. Compared with clinical drugs, **I** showed pretty good antibacterial activity. We presumed that the good lipophilic nature of **I** and the strong toxicity of Cd^{2+} ion may be responsible for the good antibacterial activities.

Keywords: crystal structure, C–H···π interaction, ferrocenyl carboxylate, antibacterial activities

DOI: 10.1134/S1070328422040078

INTRODUCTION

Metal-organic coordination complexes have attracted great attention due to their new structural topologies and potential applications as important functional materials in magnetism, luminescent materials, molecular adsorption, and semiconductors [1–5]. For construction complexes with unique structures and functions, the selection of special inorganic and organic building blocks is crucial. As an important functional ligand, ferrocene carboxylic acid and its derivatives with the strong coordination ability, various coordination modes and unique properties [6, 7] have become the preferred organic groups for the synthesis of functional complexes. And as an anionic ligand, ferrocene carboxylic acid ligand is easy to cooperate with some neutral nitrogenous ligands. By using the principle of molecular self-assembly, a large number of neutral nitrogenous ligands with different structures can be introduced, which can result in various structures. On the other hand, the prepared functional materials combine the advantages of organic ligands with metals, making these complexes potentially useful in terms of magnetic, non-linear optics, catalysis, and antibacterial activities.

According to above considerations and on the basis of previous studies, two Cd(II) complexes and a supramolecular compound have successfully obtained by using 2-chloro-4-ferrocenylbenzoic acid as anionic ligand and three nitrogen neutral ligands (Schemes 1 and 2) as second ligands. Herein, we report the syntheses, crystal structures, thermal properties of two Cd(II) complexes $[Cd(\eta^1\text{-}OOCClH_3C_6Fc)(\eta^2\text{-}OOCClH_3C_6Fc)(Phen)(H_2O)]$ (**I**), $[Cd(\eta^2\text{-}OOCClH_3C_6Fc)_2\text{-}(2,2'\text{-bipy})]$ (**II**) and the supramolecular compound $[(HOOCClH_3C_6Fc)_2(4,4'\text{-bipy})]$ (**III**). There is also the detailed discussion on various weak stacking interactions in **I**–**III**. Furthermore, the microbiological properties of **I**–**III** were studied. $FcC_6H_3ClCOOH$ and organic nitrogen-heterocyclic ligands and syntheses of **I**–**III** are listed in the Schemes 1 and 2, respectively.

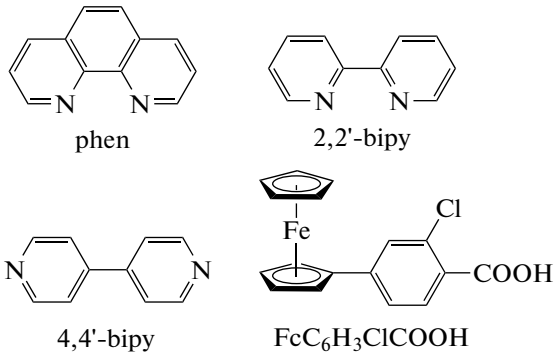

Scheme 1.

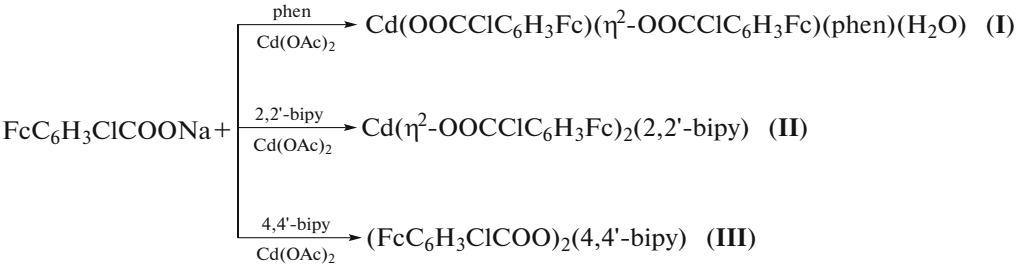

Scheme 2.

EXPERIMENTAL

Materials and methods. We prepared 2-chloro-4-ferrocenylbenzoic acid and corresponding sodium salt according to literature methods [8]. All other chemicals were obtained from commercial sources and used without further purification. The analysis of carbon, hydrogen and nitrogen was conducted on a Flash EA 1112 elemental analyzer. IR spectra were taken on a Bruker Tensor 27 spectrophotometer with KBr pellets in 400–4000 cm^{-1} region. The phase-structures of the obtained bulk samples were identified through an Powder X-ray diffraction (PXRD) instrument (D8 advance, Bruker, Germany).

Test microorganism and medium. The antibacterial effects of compounds (metal salts, free ligand, standard drug and two complexes) were screened by the agar diffusion test against two gram-positive bacteria *Bacillus subtilis* (CMCC(B)63501), *Staphylococcus aureus* (ATCC29213), two gram-negative bacteria *Escherichia coli* (ATCC25922) and *Salmonella enteritidis* (ATCC13076). The four bacterial strains were obtained from Zhengzhou University Center for Drug Evaluation and School of Life Sciences in Zhengzhou University.

Antibacterial tests. Antibacterial tests were carried out against cultures of gram-positive and gram-negative strains by the disk diffusion test on agar. The sensitivity was recorded by measuring the clear zone of growth inhibition. Besides the evaluation of the bactericidal activity by measuring the growth inhibition diameter, the minimal inhibitory concentration (MIC) using the method of progressive double dilution in liquid media by varying concentration was also determined only for compounds showing at least 0.8 mm of growth inhibition. All assays were done in triplicate and results were consistent within the experimental error.

The typical growth inhibition tests were performed by using an agar well diffusion method described by Tella and Obaleye (2010) [9]. The zones of inhibition formed were measured in mm. Finally, complexes **I** showed good antibacterial effect. On the contrary, others did not show obvious effect in the disk diffusion test, so no further determination of MIC was done for those compounds.

MIC of compounds were determined using the LB dilution method and two percent of sterile DMSO was used as a medium for MIC. An elisa 96 wells cell culture plate was used for MIC assays, and the final concentration of each compound were 128, 64, 32, 16, 8, 4, 2, 1, 0.5, 0.25 μg/mL. Subsequently, 96 wells cell culture plates were incubated in a humid chamber at 37°C for 20 h. Finally, we monitored bacterial growth by measuring turbidity of the culture. All assays were accomplished in triplicates. The MIC results are expressed as μg/mL.

Synthesis of [Cd(η^1-OOCClH$_3$C$_6$Fc)(η^2-OOCClH$_3$C$_6$Fc)(phen)(H$_2$O)] (I). The methanol solution (4 mL) of adjuvant ligand phen (9.0 mg, 0.05 mmol) was added to a methanol solution (4 mL) of $Cd(OAc)_2 \cdot 2H_2O$ (13.4 mg, 0.05 mmol), and then the methanol solution (3 mL) of $FcC_6H_4ClCOONa$ (36.7 mg,

0.10 mmol) was added to above mixture. The mixture was stirred and then filtered. Then the mixture solution was kept in the dark at room temperature for one-week, good quality red crystals were obtained from the resultant red solution. The yield was 53%.

For $C_{46}H_{34}O_6N_2Cl_2Fe_2Cd$			
Anal. calcd., %	C, 55.77	H, 3.43	N, 2.83
Found, %	C, 55.39	H, 3.41	N, 2.71

IR spectrum (KBr; ν, cm^{-1}): 3428 w, 1588 s, 1385 s, 1104 w, 1045 w, 1044 m, 852 s, 728 s, 485 s.

Synthesis of [Cd(η²-OOCClH$_3$C$_6$Fc)$_2$(2,2'-bipy)] (II) was carried by the similar procedure for **I**, and then 2,2'-bipy was used to replace phen. The final mixture was kept in the dark at room temperature. Two weeks later, good quality orange crystals steady in the air were obtained from the resultant red solution. The yield was 47%.

For $C_{44}H_{34}O_5N_2Cl_2Fe_2Cd$			
Anal. calcd., %	C, 54.67	H, 3.52	N, 2.90
Found, %	C, 54.39	H, 3.86	N 3.03

IR spectrum (KBr; ν, cm^{-1}): 3421 m, 1597 s, 1391 s, 1086 w, 1043 w, 834 w, 767 w, 487 m.

Synthesis of [(HOOCClH$_3$C$_6$Fc)$_2$(4,4'-bipy)] (III) was carried by the similar procedure for **I**, and then 4,4'-bipy was used to replace phen. The final mixture was kept in the dark at room temperature. Two weeks later, good quality yellow crystals steady in the air were obtained from the resultant red solution. The yield was 53%.

For $C_{44}H_{34}O_4N_2Cl_2Fe_2$			
Anal. calcd., %	C, 63.06	H 4.06	N, 3.34
Found, %	C, 62.95	H, 4.32	N, 3.50

IR spectrum (KBr; ν, cm^{-1}): 3444 s, 1739 m, 1710 s, 1602 s, 1409 m, 1228 m, 1088 w, 1044 m, 876 w, 488 m.

X-ray crystallography. The diffraction intensity data of **I**–**III** were collected by a Rigaku RAXIS-IV and SATURN-724 imaging plate area detector with graphite monochromated MoK_α radiation (λ = 0.71073 Å) at room temperature. The structures were solved by direct methods and expanded with Fourier techniques. The non-hydrogen atoms were refined anisotropically. Hydrogen atoms were included but not refined. The final cycle of full-matrix least-squares refinement was based on observed reflections and variable parameters. All calculations were performed by using SHELX-97 crystallographic software package [10]. Crystallographic crystal data and processing parameters for complexes **I**–**III** are showed in Table 1 and corresponding selected bond lengths and bond angles are listed in Table 2.

Supplementary material for structures **I**–**III** has been deposited with the Cambridge Crystallographic Data Centre (CCDC nos. 1874492–1874494, respectively; deposit@ccdc.cam.ac.uk or http://www.ccdc.cam.ac.uk/data-request/cif).

RESULTS AND DISCUSSION

Crystallographic analysis reveals that **I** crystallizes in the triclinic system with the $P\bar{1}$ space group. The asymmetric unit of **I** contains one Cd(II) metal center, two $FcC_6H_3ClCOO^-$ anion, one phen ligand and one water molecule (Fig. 1a). The Cd(II) metal center is in a distorted octahedron coordination linked by four O atoms (O(1), O(3), O(4)) from two $FcC_6H_3ClCOO^-$ ligands, two N atoms (N(1), N(2)) from one phen, and one O5 atom from one H_2O molecule. The Cd–O bond lengths are in the range of 2.214(2)–2.492(2) Å, the Cd(1)–N(1) and Cd(1)–N(2) distances are 2.334(2) and 2.328(2) Å, as listed in Table 2. There are intermolecular π···π stacking interactions between the centroids of pyridinyl rings and phenyl rings (Cg(1)···Cg(2)) with a distance of 3.51 Å {Cg1 = C(41)–N(2), Cg2 = C(38)–C(46)} and intermolecular C(40)$^{\#1}$–H(40)$^{\#1}$···C(l2), C(40)–H(40)···C(l2)$^{\#1}$ hydrogen bonds (H···Cl 2.829 Å, bond angles 136.59° ($^{\#1}$ $-1-x, 2-y, 2-z$) in **I**, which links two neighboring asymmetric units to generate a dinuclear secondary building unit (SBU) with Cd···Cd separation 8.565(3) Å (Fig. 1b). Analysis of the crystal packing reveals that the dinuclear SBU is further extended to 1D ribbon (Fig. 1c) along the *a* axis by the edge-to-face C–H···π interactions, the ferrocene rings act as centroids for the C–H···π interactions, namely, C(18)–H(18)···Cg3 (Cg3 = C(6)–C(10)) with a distance of 3.73 Å (dihedral angle 88.276°; H/π-plane separation 2.83 Å) [11–14]. These 1D ribbons are further extended to 3D supramolecular structure by intermolecular C–H···π interactions. There are two types of intermolecular edge-to-face C–H···π interactions: 3.72 Å (dihedral angle 88.86°; H/π-plane separation 3.00 Å) for C(3)–H(3)···Cg4 and 3.67 Å (dihedral angle 86.67°; H/π-plane separation 2.79 Å) for C(33)–H(33)···Cg5, in which ferrocene rings act as centroids (Cg4 = C(18)–C(22) ring, Cg5 = C(1)–C(5) ring). The 3D supramolecular architecture (Fig. 1d) is further reinforced through O–H···O hydrogen bonds (O(5)···O(2) 2.72 Å, bond angle 171.49°, O(5)···O(3) 2.77 Å, bond angle 155.24°).

The X-ray crystallographic analysis reveals that **II** is a 0D architecture which is similar to **I**. Complex **II** crystallizes in the orthorhombic system with the $P2_12_12_1$ space group. The asymmetric unit of complex **II** contains one Cd(II) metal center, two $FcC_6H_3ClCOO^-$ anion, one phen ligand and one water molecule (Fig. 2a). The Cd(II) metal center is in a distorted pentagonal bipyramidal coordination sphere, which is defined by one nitrogen atom (N(1)) from 2,2'-bipy

Table 1. Crystal data and structure refinement for **I**–**III**

Parameter	Value		
	I	**II**	**III**
Formula	$C_{46}H_{34}O_6N_2Cl_2Fe_2Cd$	$C_{44}H_{34}O_5N_2Cl_2Fe_2Cd$	$C_{44}H_{34}N_2O_4Cl_2Fe_2$
Formula weight	989.75	965.73	837.33
Temperature, K	293(2)	291(2)	293(2)
Wavelength, Å	0.71073	0.71073	0.71073
Crystal system	Triclinic	Orthorhombic	Monoclinic
Space group	$P\bar{1}$	$P2_12_12_1$	$P2_1/c$
a, Å	9.2343(18)	9.5266(19)	15.403(3)
b, Å	13.023(3)	9.6896(19)	10.658(2)
c, Å	17.108(3)	42.705(9)	11.825(2)
α, deg	87.66(3)	90	90
β, deg	79.08(3)	90	108.45(3)
γ, deg	74.67(3)	90	90
Volume, Å	1948.1(7)	3942.0(14)	1841.4(6)
Z	2	4	2
ρ_c, g cm^{-3}	1.687	1.627	1.510
F(000)	996	1944	860
θ range, deg	3.15–25.00	1.91–25.00	2.64–31.07
Reflections collected/unique	19499/6806	11602/6687	2495/5366
Data/restraints/parameters	6806/7/532	6687/0/506	5366/0/245
Goodness of fit on F^2	1.074	0.876	1.139
Final R_1[a], wR_2[b]	0.0313, 0.0719	0.0397, 0.0926	0.0593, 0.1371

[a] $R_1 = ||F_o|-|F_c||/|F_o|$. [b] $wR_2 = [w(|F_o^2|-|F_c^2|)^2/w|F_o^2|^2]^{1/2}$.

ligand and one oxygen atom (O(5)) from coordinated water molecule occupying the apical positions, while the basal plane is completed by four oxygen atoms (O(1), O(2), O(3), O(4)) from two different $FcC_6H_3ClCOO^-$ anion (Cd(1)–O(1) 2.366, Cd(1)–O(2) 2.535, Cd(1)–O(3) 2.332, Cd(1)–O(4) 2.487 Å) and one nitrogen atom (N(2)) of 2,2'-bipy ligand (Cd(1)–N(2) 2.372 Å) (Fig. 2a). In **II**, both of the $FcC_6H_3ClCOO^-$ anions with chelating carboxylate group coordinated with the Cd(II) metal center, 2,2'-bipy ligand also links the Cd(II) metal center by two nitrogen atoms in a chelating mode. There exist intermolecular π···π stacking interactions between the centroids of pyridinyl rings Cg1···Cg2 with a distance of 3.708 Å (dihedral angle 29.86°; Cg1 = C(35)–N(1), Cg2 = C(39)–N(2)) and intermolecular C(42)$^{\#1}$–H(42)$^{\#1}$···Cl(2), C(42)–H(42)···Cl(2)$^{\#1}$ hydrogen bonds (H···Cl 2.847 Å, bond angles 137.02° ($^{\#1}$ $-x$, $-1/2-y$, $1/2-z$) in **II**, which links two neighboring asymmetric units to generate a dinuclear SBU with Cd···Cd separation is 8.565(3) Å (Fig. 2b). There are also the C–H···π interactions with a distance of 4.18 Å (dihedral angle 83.14°; H/π-plane separation 3.28 Å) for C(19)–H(19)···Cg3 (Cg3 = C(1)–C(5)), in which the ferrocene rings act as centroids. With the above C–H···π interactions, the dinuclear SBUs are extended according b axis into 1D ribbon structure (Fig. 2c). Along the a axis, these 1D ribbons are paralleled to each other and connected through O–H···O (O(5)···O(2) 2.69 Å, bond angle 135.09°; O(5)···O(3) 2.78 Å, bond angle 150.00°) hydrogen bonds to form 2D supramolecular structure. Interestingly, the 2D supramolecular layers are further extended into 3D supramolecular structure (Fig. 2d) by C–H···π interactions.

Crystallographic analysis reveals that **III** crystallizes in the monoclinic system with the $P2_1/c$ space group. The asymmetric unit of compound III contains two $FcC_6H_3ClCOOH$ molecules and one 4,4'-bipy molecule (Fig. 3a). The dihedral angle with the benzene ring and ferrocene ring of $FcC_6H_3ClCOOH$ is about 14.71°. The 4,4'-bipy molecules show a typical planar structure. There are some interactions such as hydrogen bonds and π–π stackings exist in compound **III**, which play a crucial role in **III**. Analysis of the crystal packing of **III** revealed that an infinite 2D

Table 2. Selected bond lengths (Å) and bond angles (deg)

Complex **I**			
Bond	*d*, Å	Bond	*d*, Å
Cd(1)–O(1)	2.214(2)	Cd(1)–N(1)	2.334(2)
Cd(1)–O(5)	2.308(2)	Cd(1)–N(2)	2.382(2)
Cd(1)–O(4)	2.324(2)	Cd(1)–O(3)	2.492(2)
O(1)–Cd(1)–O(5)	93.98(10)	O(5)–Cd(1)–N(2)	112.20(8)
Angle	ω, deg	Angle	ω, deg
O(1)Cd(1)O(4)	101.20(9)	O(4)Cd(1)N(2)	100.29(8)
O(5)Cd(1)O(4)	145.39(8)	N(1)Cd(1)N(2)	70.45(8)
O(1)Cd(1)N(1)	150.17(9)	O(1)Cd(1)O(3)	123.24(8)
O(5)Cd(1)N(1)	82.33(9)	O(5)Cd(1)O(3)	91.98(8)
O(4)Cd(1)N(1)	98.25(8)	O(4)Cd(1)O(3)	53.73(7)
O(1)Cd(1)N(2)	83.91(9)	N(1)Cd(1)O(3)	86.55(8)
Complex **II**			
Bond	*d*, Å	Bond	*d*, Å
Cd(1)–O(5)	2.297(4)	Cd(1)–O(1)	2.366(4)
Cd(1)–O(3)	2.332(4)	Cd(1)–N(2)	2.372(4)
Cd(1)–N(1)	2.357(5)	Cd(1)–O(4)	2.487(4)
Cd(1)–O(2)	2.535(5)	O(3)–Cd(1)–O(1)	131.48(15)
Angle	ω, deg	Angle	ω, deg
O(5)Cd(1)O(3)	98.90(16)	N(2)Cd(1)(1)	81.97(18)
O(5)Cd(1)N(2)	92.96(15)	O(5)Cd(1)N(1)	161.87(16)
O(3)Cd(1)N(2)	145.25(17)	O(3)Cd(1)N(1)	98.80(18)
O(5)Cd(1)O(1)	84.26(15)	N(1)Cd(1)O(4)	107.20(17)
N(2)Cd(1)N(1)	70.07(17)	O(5)Cd(1)O(2)	105.49(17)
O(1)Cd(1)N(1)	86.97(18)	O(3)Cd(1)O(2)	80.36(14)
O(5)Cd(1)O(4)	80.43(15)	N(2)Cd(1)O(2)	127.57(16)
O(3 Cd(1)O(4)	53.76(12)	O(1)Cd(1)O(2)	52.75(15)
N(2)Cd(1)O(4)	96.91(15)	N(1)Cd(1)O(2)	81.37(18)
O(1)Cd(1)O(4)	164.58(15)	O(4)Cd(1)O(2)	133.93(13)

supramolecular structure (Fig. 3b) was formed by π–π stacking interactions between benzene rings of $FcC_6H_3ClCOOH$ and pyridine rings of 4,4'-bipy with interplanar separation of 3.33 Å (center-to-center separations 3.86 Å) [15–17]. Meanwhile, the O–H···N hydrogen bond (O···N 2.63 Å, bond angle 172.85°) between adjacent ferrocene and 4,4'-bipy also exists to further stabilize it. Finally, these weak interactions (Fig. 3c) extend the structure to a 3D supramolecular structure.

PXRD experiments were also carried out to confirm the phase purities of complexes **I** and **II**. The experimental and structure-simulated PXRD patterns of the two complexes are compared (Fig. 4). The main peaks of **I** and **II** and the simulated match well, indicating the purities of the two compounds.

Antibacterial activities of **I**–**III**, their corresponding ligand and metal salts were tested against *S. aureus*, *E. coli, B. subtillis* and *S. enteritidis* bacteria using the agar well diffusion method [18, 19]. Compound **III**, the ligands $FcC_6H_3ClCOOH$, phen and 2,2'-bipy, DMSO and metal salts exhibit inactivity against *S. aureus*, *E. coli, B. subtillis* and *S. enteritidis* bacteria. Complex **I** exhibited the better activity against *S. aureus*, *E. coli* and *B. subtillis*. Meanwhile, **II** also showed activity against *B. subtillis*. To compare their antimicrobial activities, the MIC values of **I** and **II** were also determined, meanwhile, some commercially drugs [20–22] in Table 3 were also used as the avail-

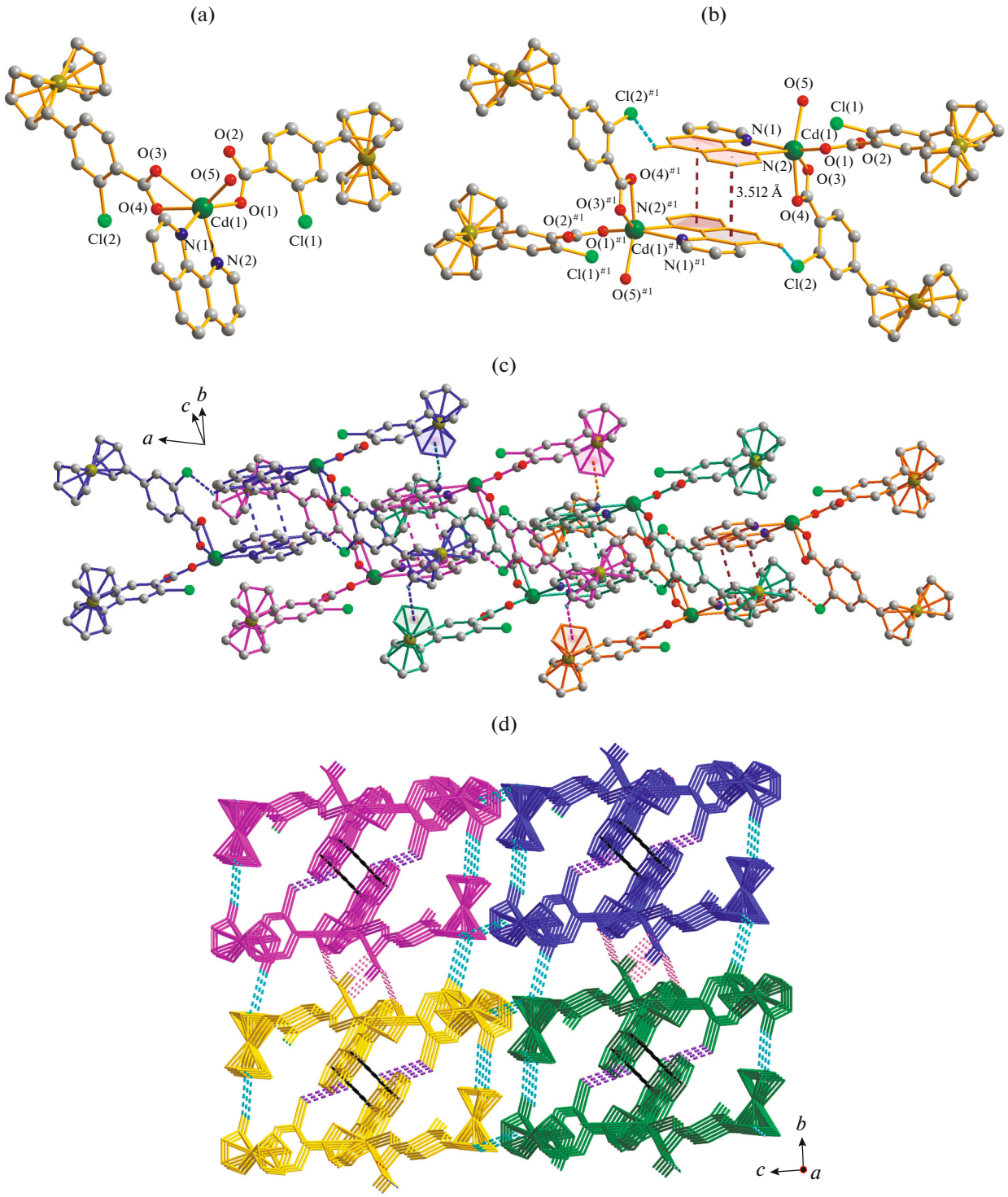

Fig. 1. View of the asymmetric unit of complex **I** (the hydrogen atoms have been omitted for clarity) (a); 1D paddle-shaped chain of $[Cd(\eta^2\text{-}OOCClH_3C_6Fc)_2(phen)]_n$ (b); two neighboring 1D chains with different Cd centers are connected into 1D ribbon structure by weak C–H···Cl and C–H···π stacking interactions (dashed lines) (c); 3D supramolecular network of **I** (the dashed lines represent weak interactions, hydrogens and solvent molecules are omitted for clarity) (d).

able standards. As shown in Table 3, **I** showed MIC value of 0.5 μg/mL towards *S. aureus* and *E. coli*, and 1 μg/mL towards *B. subtillis* which has the stronger activity than the standard drugs and other complexes against *S. aureus*, *E. coli* and *B. subtillis*. Complex **II** showed MIC value of 1 μg/mL towards *B. subtillis*. In

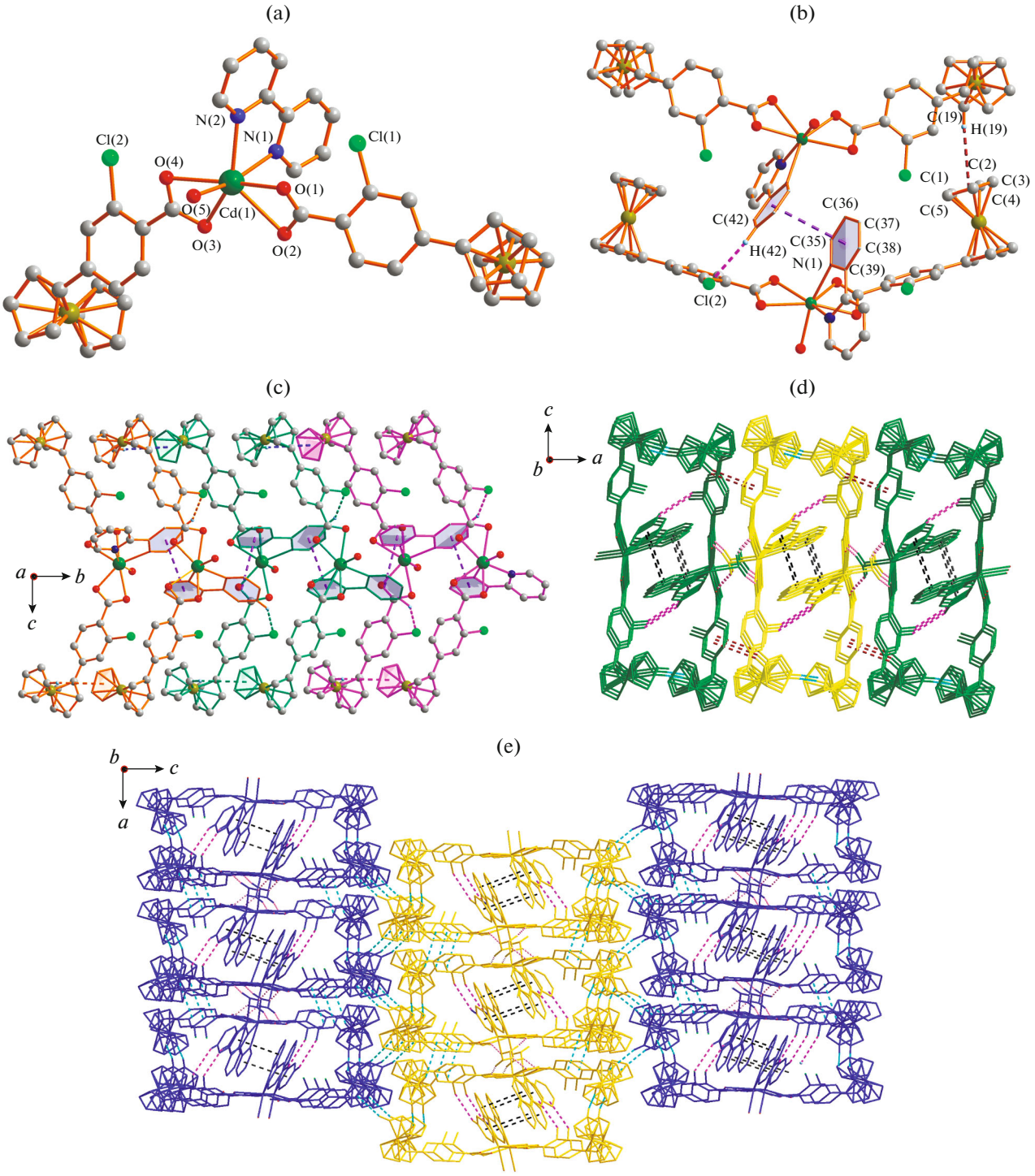

Fig. 2. Notice the weak C–H···Cl hydrogen bonds and C–H···π stacking interactions in 1D ribbon structure (partial FcC_6H_3Cl-COO^- units and hydrogen atoms are omitted for clarity) (a); notice the weak C–H···π stacking interactions between 1D ribbon structures (partial Bbbm units are omitted for clarity) (b); 2D supramolecular structure of 2 (c); 3D supramolecular network of **II** (the dashed lines represent weak interactions, hydrogens and solvent molecules are omitted for clarity) (d) and (e).

general, the antibacterial activity of **I**, **II** may be explained on the basis of chelation theory where chelation reduces the polarity of the metal atom mainly because of partial sharing of its positive charge with the donor groups and possible π-electron delocalization within the whole chelate ring [23, 24]. Additionally, chelation increases the lipophilic nature of the central atom which subsequently favours its perme-

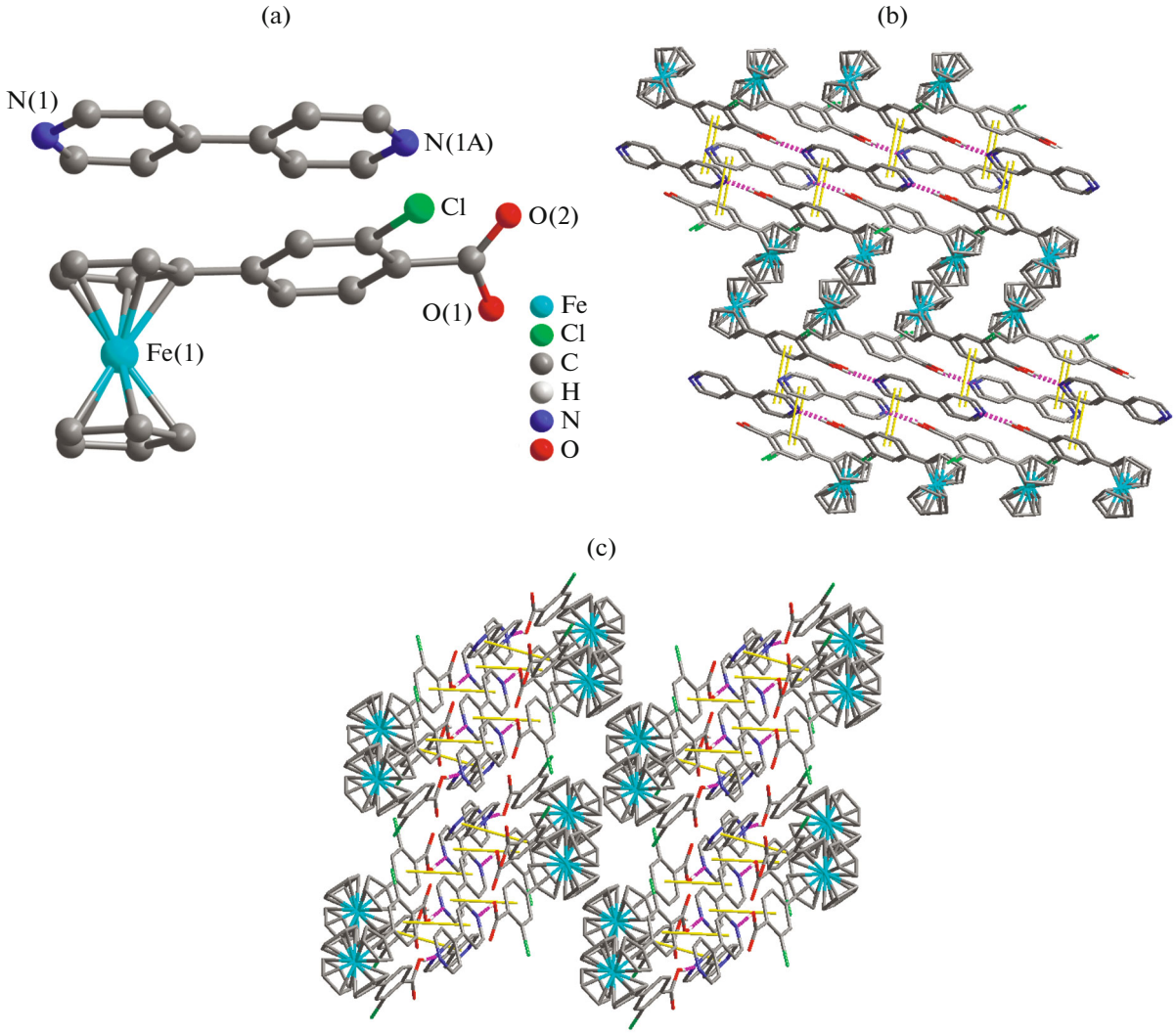

Fig. 3. Notice the weak C–H···Cl hydrogen bonds and π–π stacking interactions in 1D ribbon structure (partial $FcC_6H_3ClCOO^-$ units and hydrogen atoms are omitted for clarity) (a); notice the weak O–H···N stacking interactions between 1D ribbon structures (partial Bbbm units are omitted for clarity) (b); 3D supramolecular structure of **III** (c).

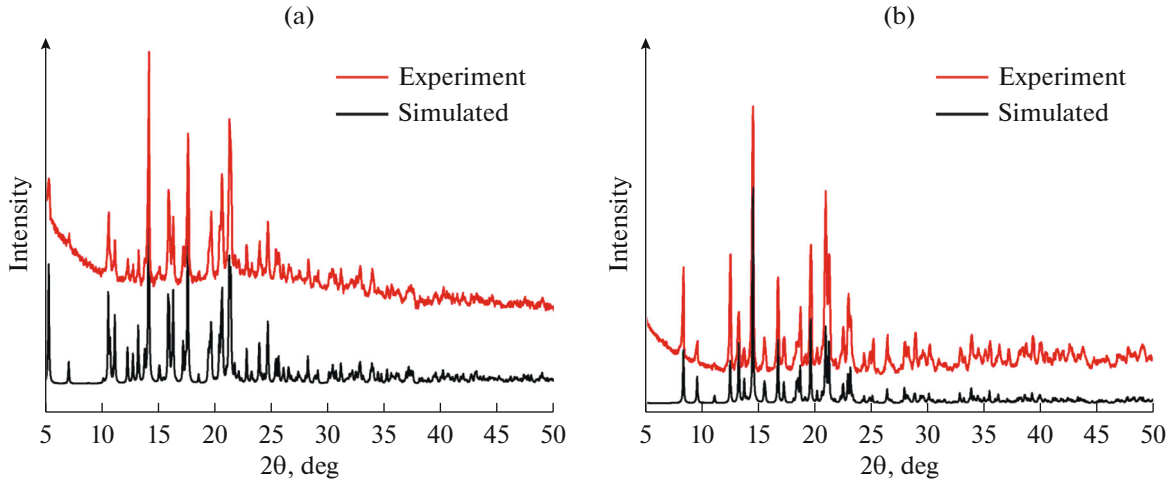

Fig. 4. PXRD patterns of **I** (a) and **II** (b).

Table 3. MIC of **I**, **II**, free ligand and clinical drugs against growth of bacteria (μg/mL)

Compounds and standards	*Staphylococcus aureus*	*Escherichia coli*	*Bacillus subtilis*	*Salmonella enteritidis*
I	0.5	0.5	1	
II			1	
$FcC_6H_3ClCOOH$	64	64	64	64
Kanamycin [17]	3.0	3.8		
Streptomycin [18]	15	20	10	
Gatifloxacin [19]	5.1	2.9	4.0	
Norfloxacin [19]	2.5	2.8	2.5	
Ciprofloxacin [19]	1.1	1.6	1.4	

ation through the lipid layer of cell membranes [25–27]. By comparing the results of antibacterial activity of **I** and **II** having the same structure and the same Cd^{2+} ion, **I** has the better activities and **II** showed inactivity against *S. aureus* and *E. coli*. phen has the bigger π-electron delocalization than 2,2'-bipy that increases the lipophilic nature of **I**, which may be one of the reasons why **I** has the higher antimicrobial activity. Also, it should be pointed out that Cd^{2+} ion with the feature of strong toxicity on animal tissues and organs threat the ecological environment and human health seriously.

FUNDING

We are thankful for financial support from National Natural Science Foundation of China (no. J1210060), Science and Technology Research Program of Henan Province of China (nos. 212102210655, 172102210483), Natural Science Foundation of Henan Province of China (no. 182300410216), Central Plains Science and Technology Innovation Leader Project of Henan Province of China (no. 214200510006), Science and Technology Innovation Talent Plan of Universities of Henan Province of China (no. 174200510018), Key Scientific Research Projects of Colleges and Universities of Henan Province of China (no. 20A150012) and Research and Cultivation Fund Project of Henan University of Engineering (no. PYXM202008).

CONFLICT OF INTEREST

The authors declare that they have no conflicts of interest.

REFERENCES

1. Guillermo, M.E. and Eugenio, C., *Chem. Soc. Rev.*, 2018, vol. 43, p. 533.
2. Cui, Y.J., Yue, Y.F., Qian, G.D., et al., *Chem. Rev.*, 2012, vol. 112, p. 1126.
3. Anastasios, I.S., *J. Am. Chem. Soc.*, 2004, vol. 126, p. 1356.
4. Li, J.P., Li, B.J., Pan, M.T., et al., *Cryst. Growth Des.*, 2017, vol. 17, p. 2975.
5. Yu, T.T., Wang, S.M., Li, X.M., et al., *CrystEngComm*, 2015, vol. 18, p. 1350.
6. Zheng, G.L., Ma, J.F., Su, Z.M., et al., *Angew. Chem., Int. Ed.*, 2004, vol. 43, p. 2409.
7. Sun, H., Zhang, Y.N., Si, X.Q., et al., *Synth. React. Inorg. Met.-Org. Nano-Met. Chem.*, 2013, vol. 43, p. 739.
8. Li, J.P., Li, L.K., Hou, H.W., et al., *Cryst. Growth Des.*, 2009, vol. 9, p. 4504.
9. Tella, A.C. and Obaleye, J.A., *Orbital Elec. J. Chem.*, 2010, vol. 2, p. 11.
10. Sheldrick, G.M., *SHELX-97, Program for the Solution and Refinement of Crystal Structures,* Göttingen: Univ. of Göttingen, 1997.
11. Cheng, J.J., Wang, S.M., Shi, Z., et al., *Inorg. Chim. Acta*, 2016, vol. 453, p. 86.
12. Duan, Y.Q., Huang, J.H., Liu, S.C., et al., *Inorg. Chem. Commun.*, 2017, vol. 81, p. 47.
13. Li, Y.L., Wang, J., Shi, B.B., et al., *Supramol. Chem.*, 2015, vols. 7–8, p. 640.
14. Zhang, Q.K., Yue, C.P., Zhang, Y., et al., *Inorg. Chim. Acta*, 2018, vol. 473, p. 112.
15. Black, A.J., Baum, G., Champness, N.R., et al., *Dalton Trans.*, 2000, p. 4285.
16. Li, J.P., Wang, X.T., Li, R.Y., et al., *Crystal Growth Des.*, 2019, vol. 19, p. 3785.
17. Wang, X.T., Li, R.Y., Zheng, X.Y., et al., *J. Mol. Struct.*, 2019, vol. 1184, p. 503.
18. Hao, Y.P., Yue, C.P., Jin, B.N., et al., *Polyhedron*, 2017, vol. 139, p. 296.
19. Patel, M.N., Dosi, P.A., and Bhatt, B.S., *Polyhedron*, 2010, vol. 29, p. 3238.

20. Salehi, M., Rahimifar, F., Kubicki, M., et al., *Inorg. Chim. Acta*, 2016, vol. 443, p. 28.

21. Surati, K.R., *Spectrochim. Acta, Part A*, 2011, vol. 79, p. 272.

22. Patel, M.N., Dosi, P.A., and Bhatt, B.S., *Polyhedron*, 2010, vol. 29, p. 3238.

23. Ye, R.P., Yang, J.X., Zhang, X., et al., *J. Mol. Struct.*, 2016, vol. 1106, p. 192.

24. Tabrizi, L., McArdle, P., Ektefan, M., et al., *Inorg. Chim. Acta*, 2016, vol. 439, p. 138.

25. Singh, D.P., Malik, V., Kumar, K., et al., *Spectrochim. Acta, Part A*, 2010, vol. 76, p. 45.

26. Caudhary, A. and Singh, R.V., *Phosphorus Sulfur Silicon Relat. Elem.*, 2003, vol. 178, p. 603.

27. Mahmoud, W.H., Deghadi, R.G., and Mohamed, G.G., *Appl. Organomet. Chem.*, 2016, vol. 30, p. 221.